Supplementary Information

Boosting the Supercapacitor Performance of Activated Carbon by Constructing Overall Conductive Networks Using Graphene Quantum Dots

Yan Qing,[†, a] Yuting Jiang,[†, b] He Lin,[a] Luxiang Wang,[a] Anjie Liu,[a] Yali Cao,[a] Rui Sheng,[a] Yong Guo,[a] Chengwei Fan,[a] Su Zhang,*[, a] Dianzeng Jia,*[, a] Zhuangjun Fan*[, b, c]

[a] Key Laboratory of Energy Materials Chemistry, Ministry of Education; Key Laboratory of Advanced Functional Materials, Autonomous Region; Institute of Applied Chemistry, Xinjiang University, Urumqi, 830046, P. R. China.

[b] College of Material Science and Chemical Engineering, Harbin Engineering University, Harbin 150001, P. R. China.

[c] School of Materials Science and Engineering, China University of Petroleum, Qingdao, 266580, P. R. China.

[†] Authors with equal contributions to this work.

1. Calculation of percentage of the GQD derived carbon in the GEAC.

According to the TG curve of the as-prepared GQDs [***Carbon***, 2018, 129, 54], the mass residual of the GQDs after carbonization at 800 °C is 43%. We also measured the mass residual of pure D (+)-glucosamine hydrochloride through hydrothermal and carbonization treatment without the GQDs at the same condition described in the experimental section. The mass residual is ca. 17.5 % after hydrothermal treatment and 10.5 % after carbonization versus the precursor D (+)-glucosamine hydrochloride. Therefore, the GEAC-0.5 contains about 67.2% carbon derived from the GQDs and 32.8% carbon from D (+)-glucosamine hydrochloride.

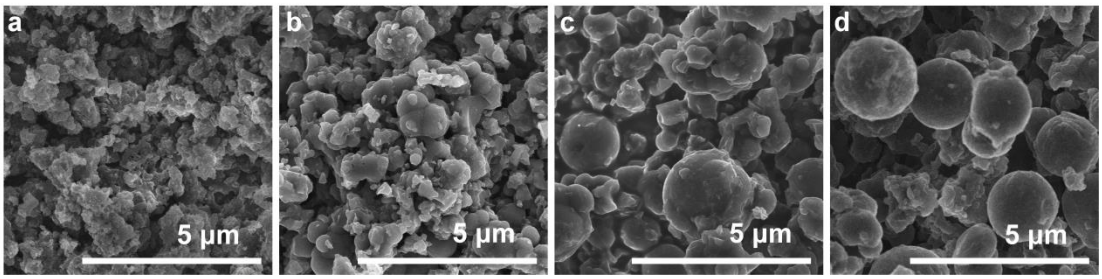

Figure S1 SEM images of the (a) AC, (b) GEAC-0.1, (c) GEAC-0.35, and (d) GEAC-0.5.

Table S1 Related concentrations of carbon and oxygen in the AC and GEAC from survey XPS spectra, and contribution of the components in the area of the XPS C_{1s} spectra.

Sample name	Concentration (at. %)		Contribution of the components in C_{1s} spectra (%)		
	C	O	C=C	C-O	C=O
AC	90	10	73	22	5
GEAC	90	10	75	20	5

Table S2 Texture properties of the AC, GEAC, GAC, and Commercial activated carbon measured by N_2 adsorption-desorption isotherms.

Sample name	S_{BET}[a] ($m^2 g^{-1}$)	V_{total}[b] ($cm^3 g^{-1}$)	V_{micro}[c] ($cm^3 g^{-1}$)	V_{meso}[d] ($cm^3 g^{-1}$)	V_{mirco}/V_{meso}
AC	2710	1.265	1.104	0.161	6.857
GEAC	2829	1.265	1.166	0.099	11.778
GAC	1742	0.749	0.421	0.328	1.284
Commercial activated carbon	1600	--	--	--	--

[a] Specific surface area calculated by BET method.

[b] Total pore volume.

[c] Volume of microspores.

[d] Volume of mesopores.

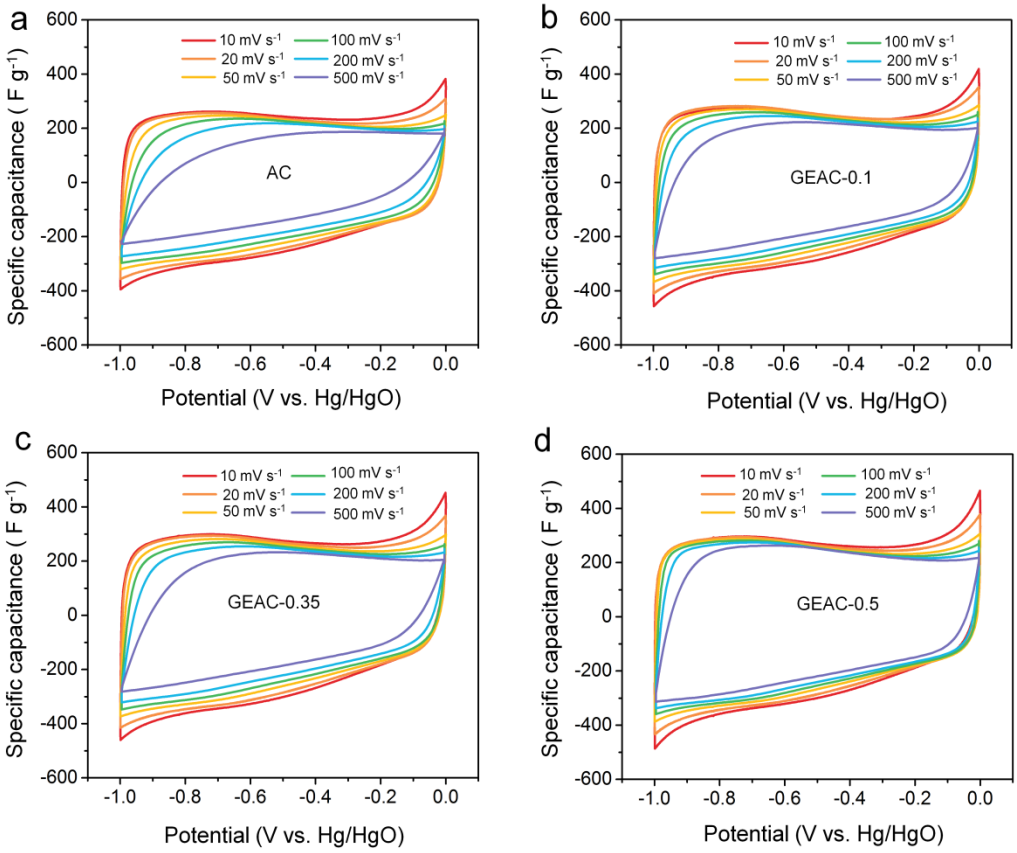

Figure S2 CV curves of the (a) AC, (b) GEAC-0.1, (c) GEAC-0.35, and (d) GEAC-0.5 at various scan rates in three-electrode system.

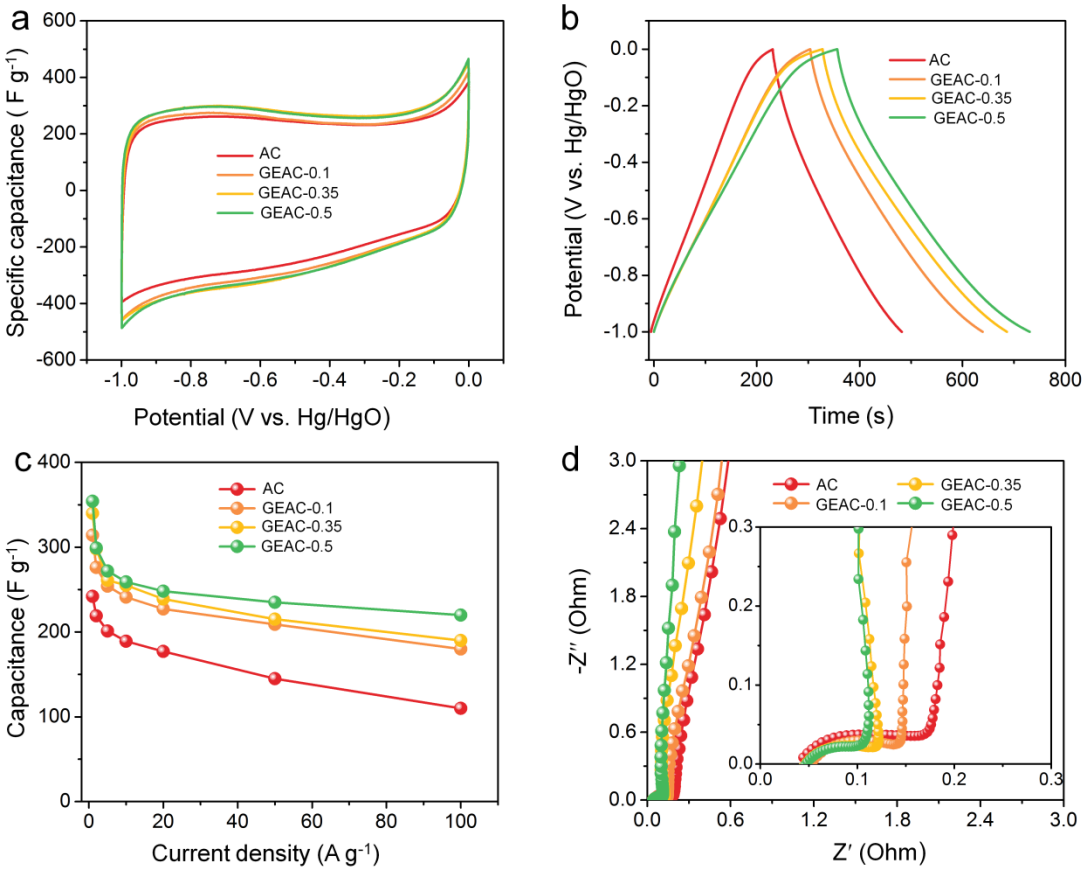

Figure S3 Electrochemical performance of the AC and GEACs measured by three-electrode system: (a) CV curves at 10 mV s^{-1}. (b) Galvanostatic charge-discharge curves at 1 A g^{-1}. (c) The rate performance at various current densities. (d) The EIS plots.

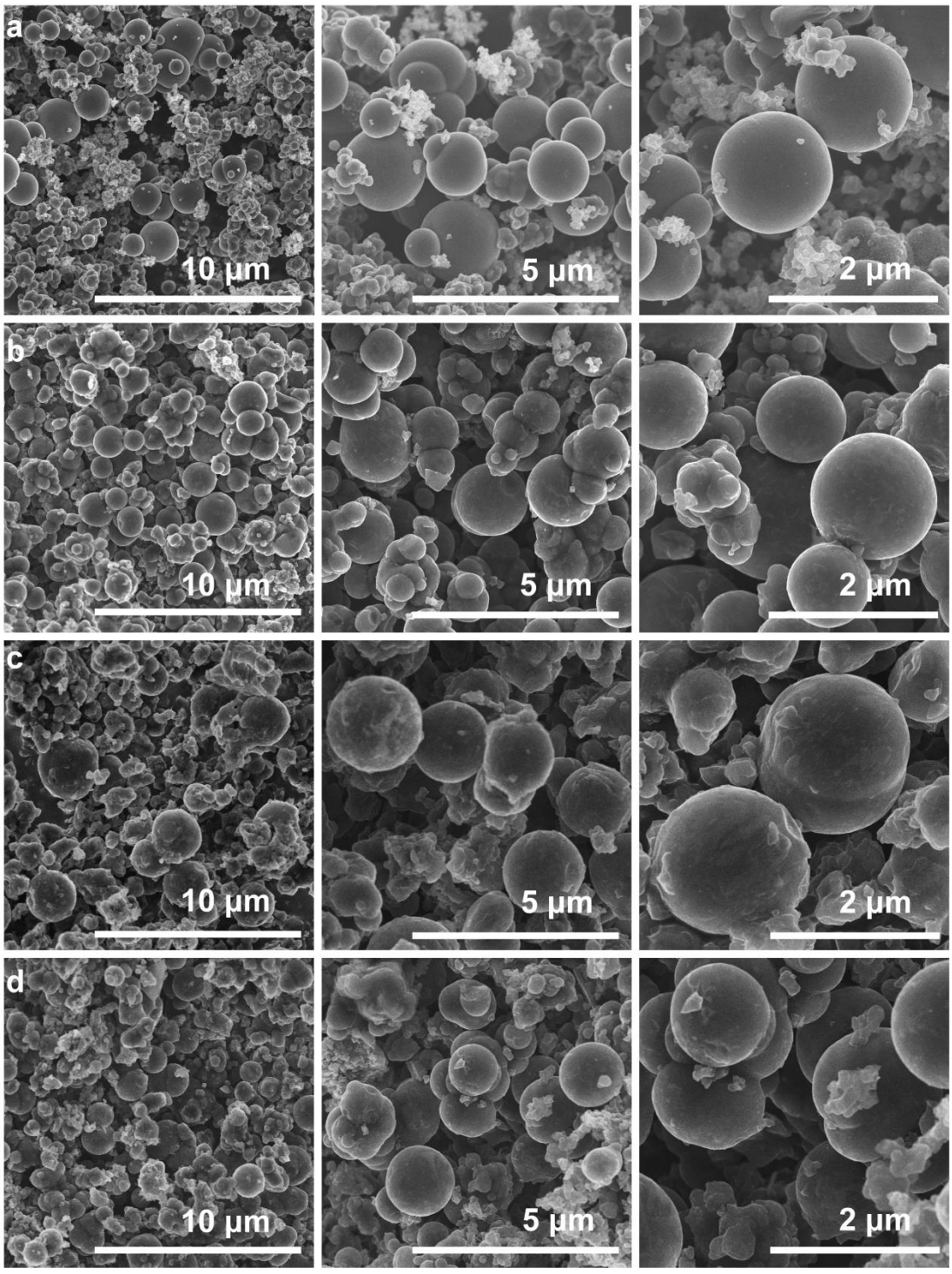

Figure S4 SEM images of the GEACs prepared by activation using different amount of KOH. The sample is named as GEAC-ratio, in where the "ratio" stands for the pre-carbonized GEAC to KOH mass ratio: (a) GEAC-1: 0, (b) GEAC-1: 2, (c) GEAC-1: 4, and (d) GEAC-1: 6.

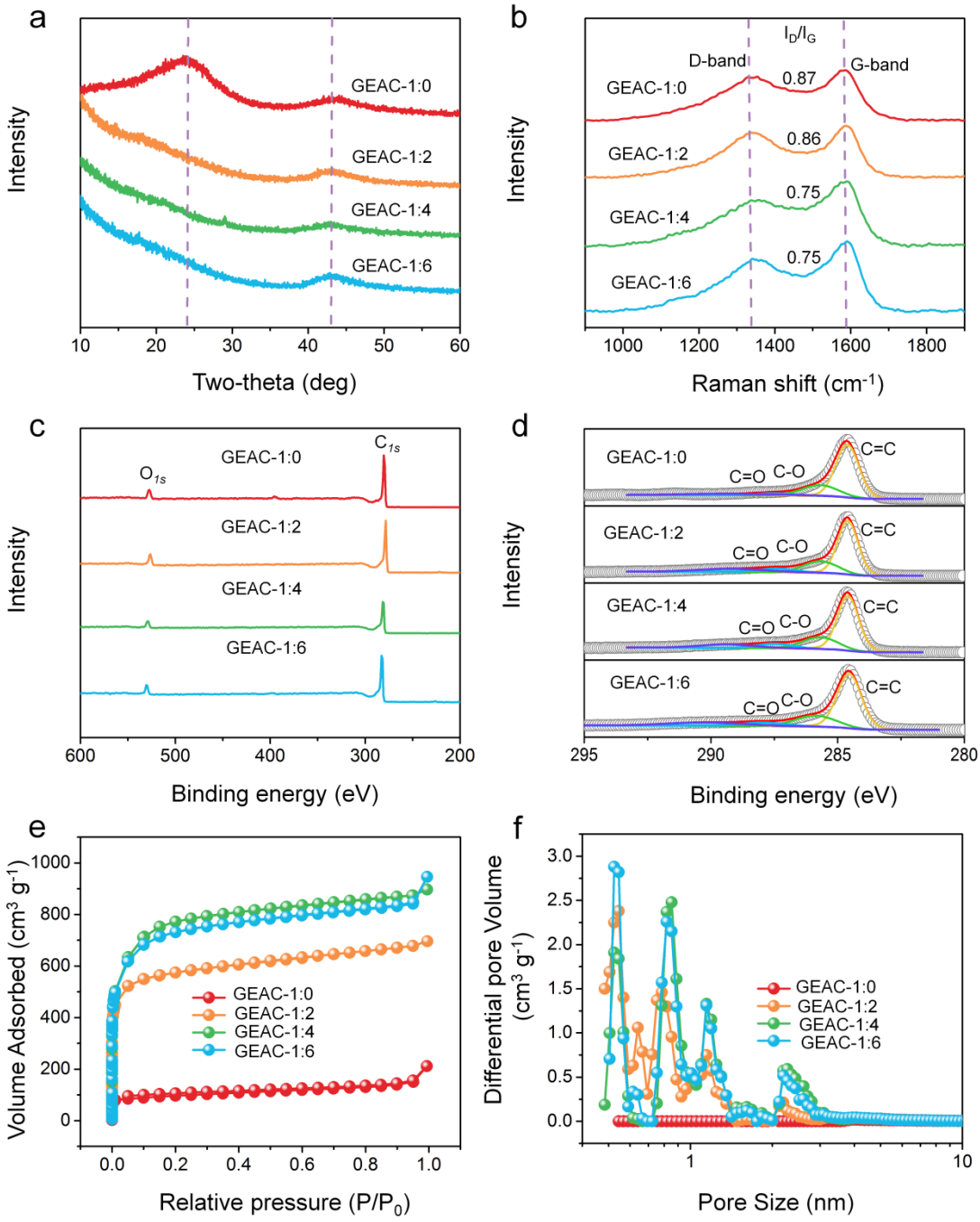

Figure S5 (a) XRD, (b) Raman, (c) XPS survey spectra, (d) XPS C_{1s} spectra, (e) N_2 adsorption-desorption isotherms, and (f) pore size distributions of the GEAC-1: 0, GEAC-1: 2, GEAC-1: 4, and GEAC-1: 6.

Table S3 Related concentrations of carbon and oxygen in the GEAC-1: 0, GEAC-1: 2, GEAC-1: 4, and GEAC-1: 6 from XPS survey spectra, and contribution of the components in the area of the XPS C_{1s} spectra.

Sample name	Concentration (at. %)		Contribution of the components in C_{1s} spectra (%)		
	C	O	C=C	C-O	C=O
GEAC-1: 0	87	13	75	21	4
GEAC-1: 2	90	10	75	20	5
GEAC- 1: 4	90	10	75	20	5
GEAC- 1: 6	90	10	82	16	2

Table S4 Texture properties of the GEAC-1: 0, GEAC-1: 2, GEAC-1: 4, and GEAC-1: 6 measured by N_2 adsorption-desorption isotherms.

Sample name	S_{BET}[a] ($m^2 g^{-1}$)	V_{total}[b] ($cm^3 g^{-1}$)	V_{mirco}[c] ($cm^3 g^{-1}$)	V_{meso}[d] ($cm^3 g^{-1}$)	V_{mirco}/V_{meso}
GEAC-1: 0	357	0.267	0.151	0.116	1.302
GEAC-1: 2	2189	0.971	0.874	0.097	9.010
GEAC-1: 4	2829	1.565	1.166	0.099	11.778
GEAC-1: 6	2906	1.262	1.194	0.068	17.559

[a] Specific surface area calculated by BET method.

[b] Total pore volume.

[c] Volume of micropores.

[d] Volume of mesopores.

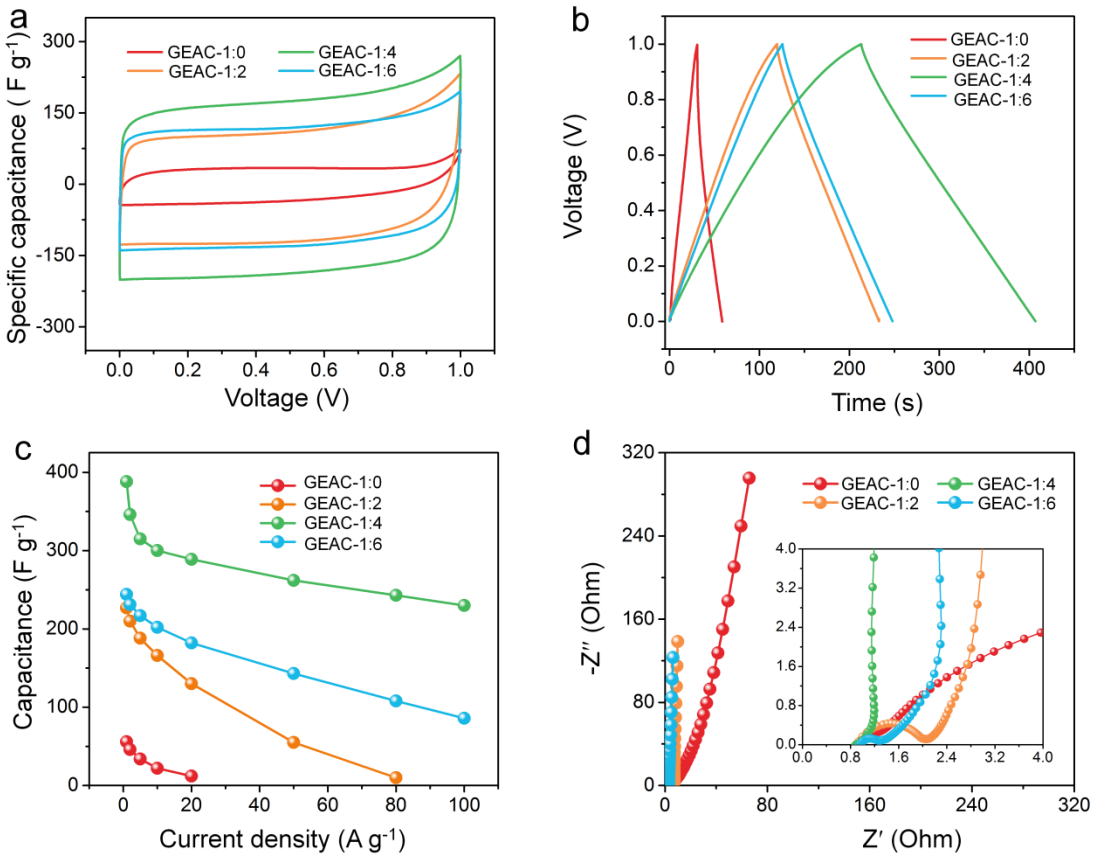

Figure S6 Electrochemical performance of the samples measured by two-electrode system: (a) CV curves at 10 mV s^{-1}, (b) Galvanostatic charge-discharge curves at 1 A g^{-1}, (c) rate performances, and (d) the EIS plots of the GEAC-1: 0, GEAC-1: 2, GEAC-1: 4, and GEAC-1: 6.

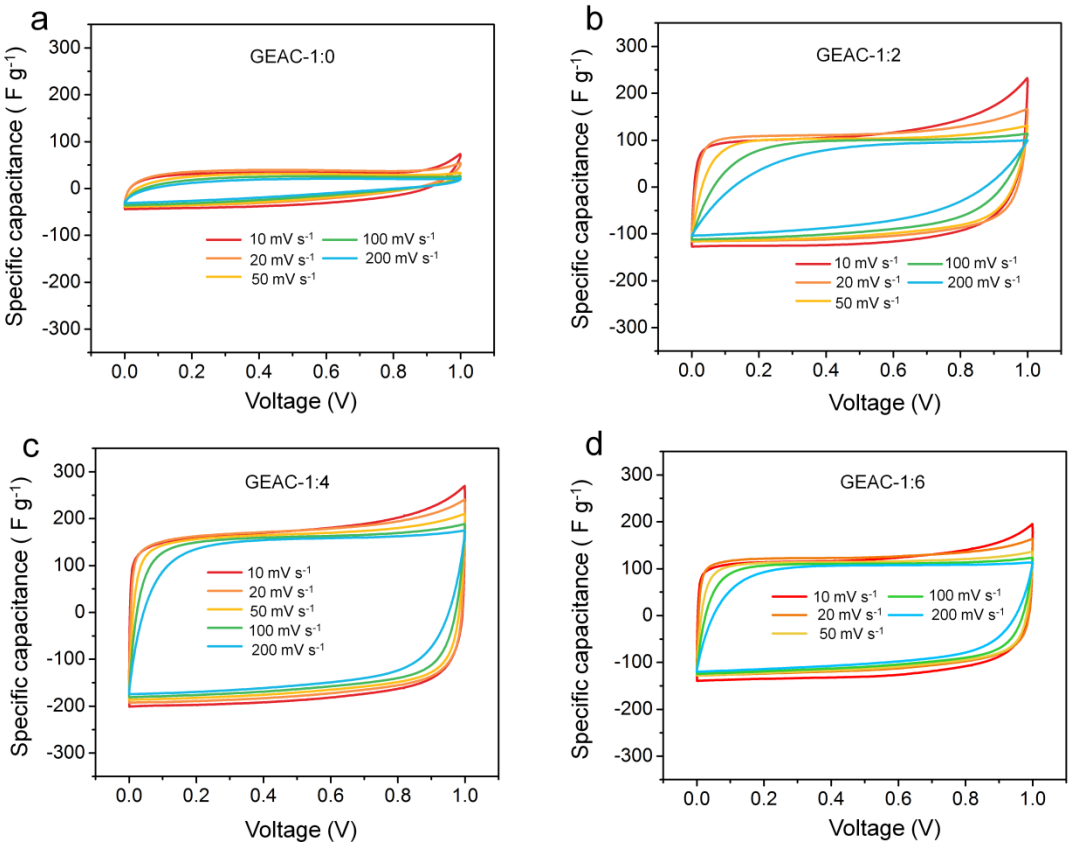

Figure S7 CV curves of (a) GEAC-1: 0, (b) GEAC-1: 2, (c) GEAC-1: 4, and (d) GEAC-1: 6 at various scan rates in two-electrode system.

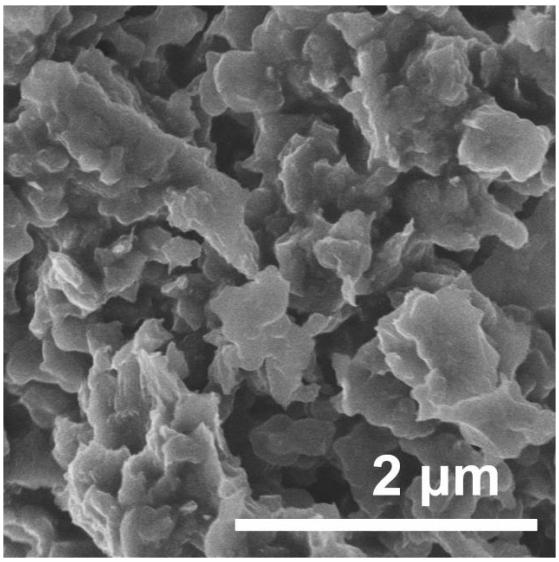

Figure S8 SEM images of the GAC.

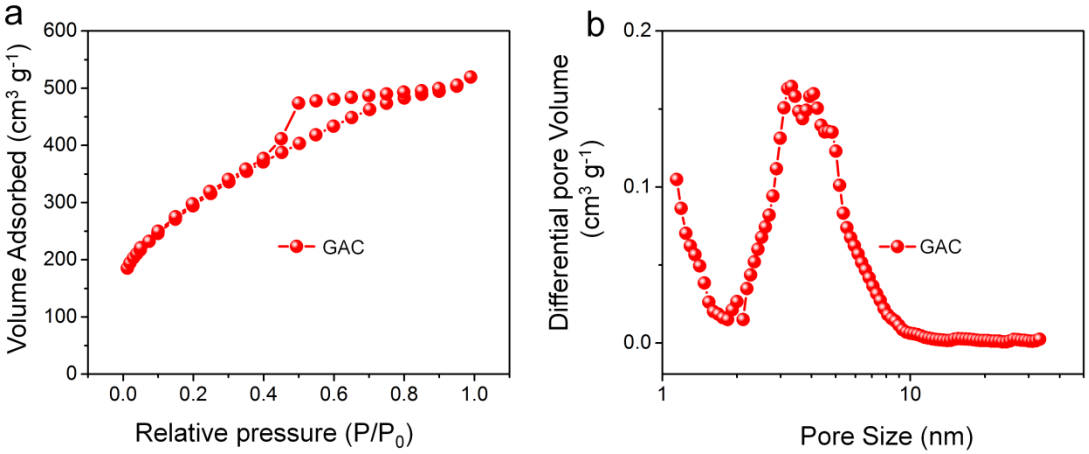

Figure S9 (a) N_2 adsorption-desorption isotherms, and (b) pore size distributions of the GAC.

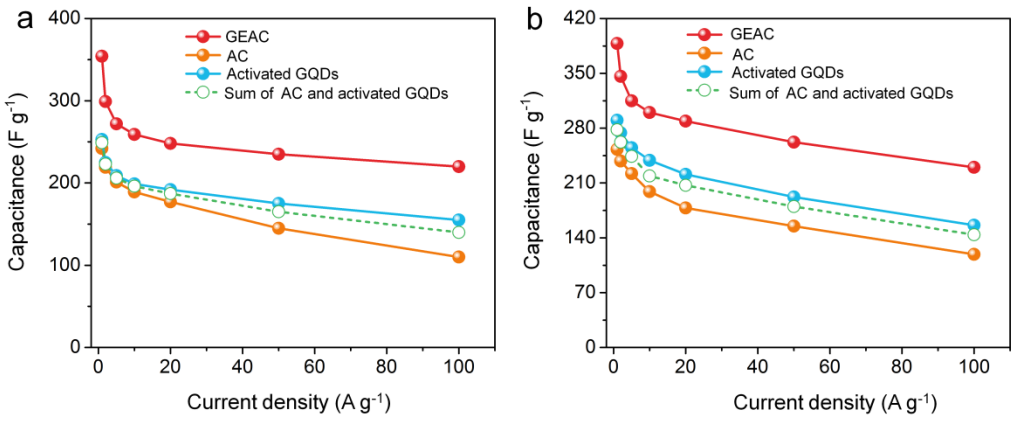

Figure S10 The rate performance of the GEAC, AC, and activated GQDs at various current densities measured by (a) three-electrode system and (b) two-electrode system.

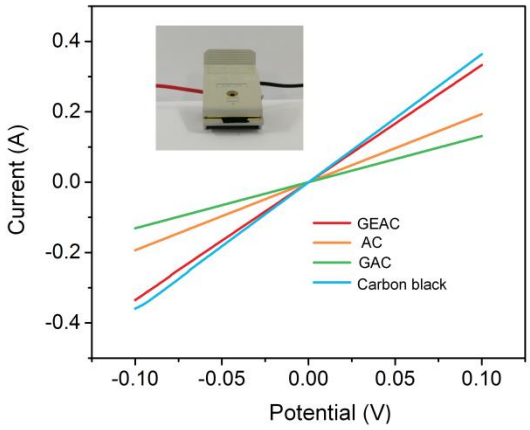

Figure S11 I-V curves of GEAC, AC, GAC, and conductive carbon black: the inserted image in shows the measurement apparatus for the conductivity test.

To evaluate the conductivity under practical application condition, we have measured the conductivity of the samples using the electrode type. Briefly, the test samples (GEAC, AC, GAC, and conductive carbon black) were homogeneously mixed with the binder (polyteteafluoroethlene, PTFE) with the mass ratio of 95:5 in ethanol by vigorous stirring and sonication, then pressed to a thin platelet and fully dried at 80 °C in vacuum. The I-V curves were carried out by the electrochemical working station (CHI660E) using the electrode clamp shown in **Figure S11**. The conductivity was calculated by the equation $\boldsymbol{\rho=R\times S/l}$ and $\boldsymbol{\sigma=1/\rho}$, where **R** is the electric resistance (Ω), **l** is the thickness of the tested platelet (m), **S** is the contact area. The conductive carbon black is ca. 105 S m^{-1}, which is much lower than its theoretical conductivity of ca. 5500 S m^{-1} possibly due to contact resistance during testing and the presence of the insulating binder. The conductivity of GEAC, AC, and GAC is 84, 39, and 29 S m^{-1}, respectively.

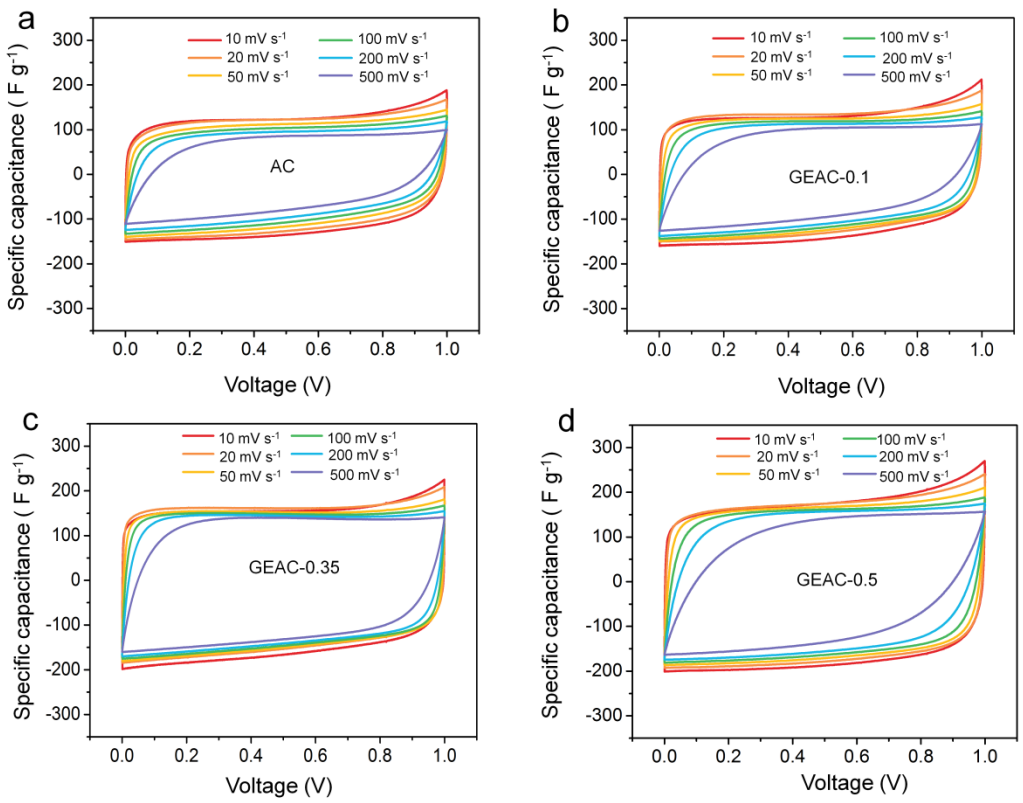

Figure S12 CV curves of the (a) AC, (b) GEAC-0.1, (c) GEAC-0.35, and (d) GEAC-0.5 at various scan rates in two-electrode system.

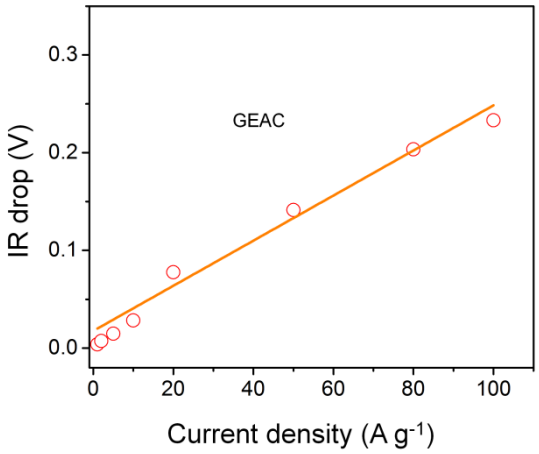

Figure S13 IR drop of the GEAC at various current densities.

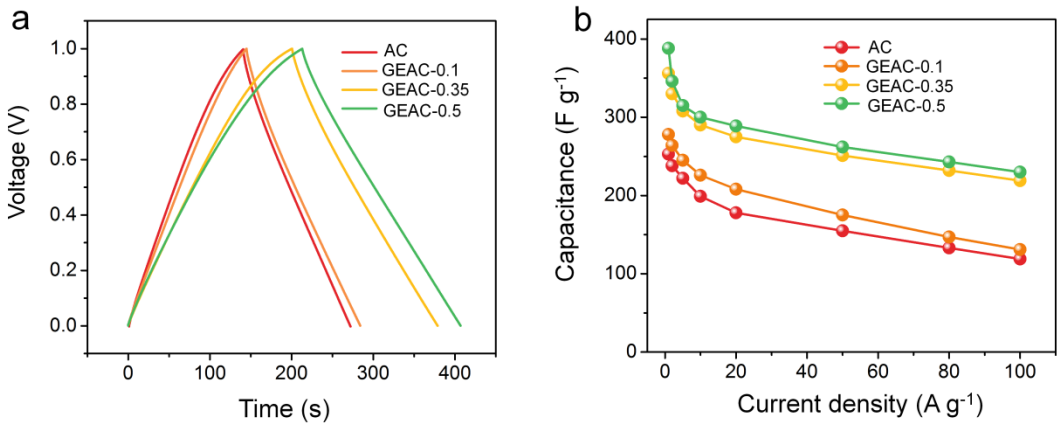

Figure S14 Electrochemical performance of the samples measured by two-electrode system: (a) Galvanostatic charge-discharge curves at 1 A g^{-1} and (b) rate performance of the AC and GEACs at various current densities.

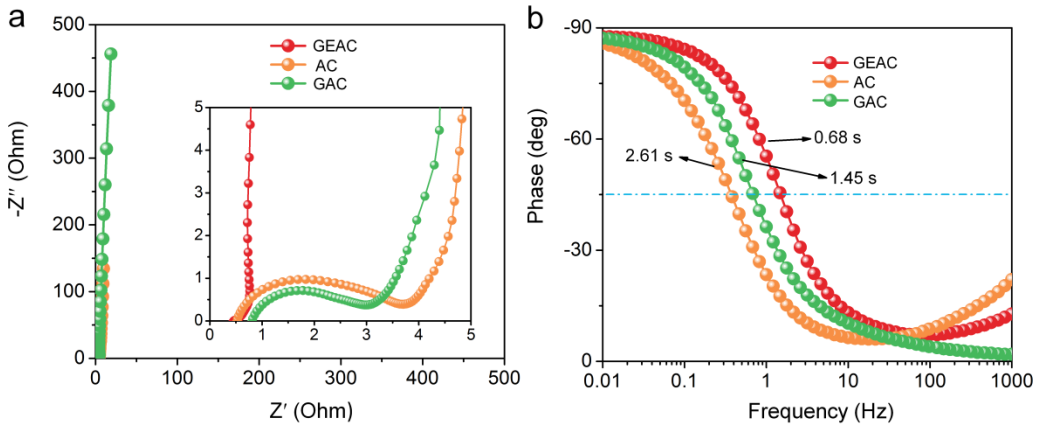

Figure S15 (a) The EIS plots and (b) Bode plots of the GEAC, AC and GAC in two-electrode system.

From the intersections of the real axis, the GEAC presents the lowest electric resistance of 0.47 Ω among the samples (0.52 Ω for the AC and 0.84 Ω for the GAC). Moreover, the GEAC also presents the smallest charge-transfer resistance (R_{ct}) of ca. 0.1 Ω among all the samples (3.2 Ω for the AC and 2.2 Ω for the GAC), indicating the robust electrochemical kinetics. In the Bode phase diagram (Figure S15b), the phase angle at 0.01 Hz is close to -90°, revealing the nearly ideal capacitive behavior. The relaxation time constant τ_0 characterized from the phase angle of -45° ($\tau_0 = 1/f_0$) of the GEAC is 0.68 s, which is considerably smaller than 2.61 s for the AC and 1.45 s for the GAC, demonstrating that constructing overall conductive networks by the highly crystallized GQDs can significantly improve the fast response ability of the activated carbon.

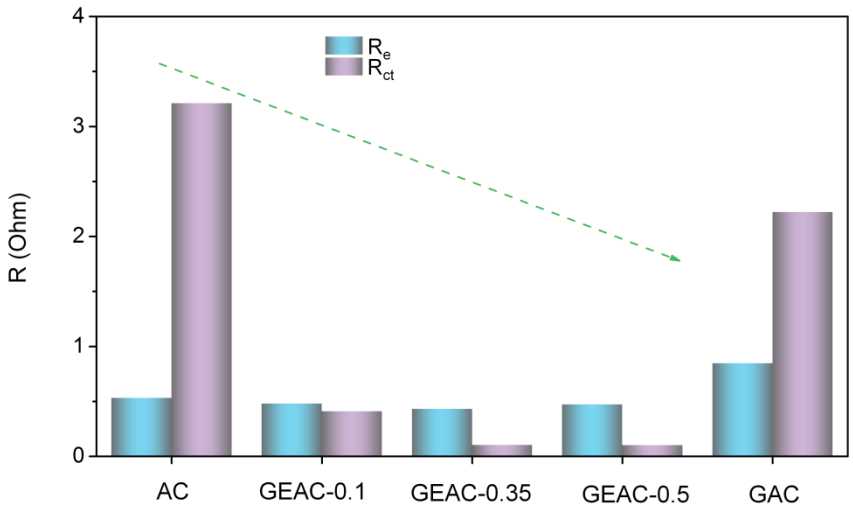

Figure S16 The calculated electric resistance (R_e) and charge-transfer resistance (R_{ct}) of the samples measured by two-electrode system.

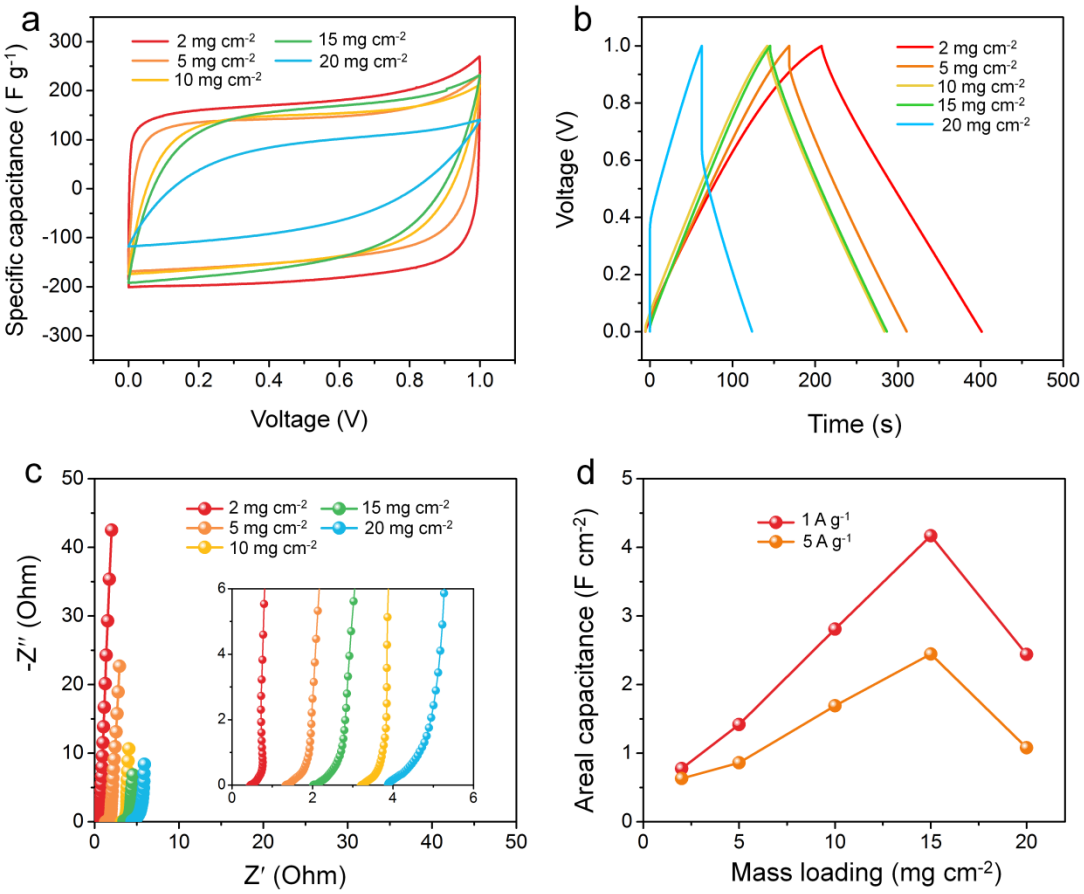

Figure S17 Electrochemical performance of the GEAC with different mass loadings on one electrode (1 cm^2) measured by two-electrode system: (a) CV curves at 10 mV s^{-1}. (b) Galvanostatic charge-discharge curves at 1 A g^{-1}. (c) The EIS plots. (d) Areal capacitances.